Strong-coupling quantum thermodynamics far from equilibrium: Non-Markovian transient quantum heat and work

Wei-Ming Huang[1] and Wei-Min Zhang [1,2,*]

[1]*Department of Physics and Center for Quantum Information Science, National Cheng Kung University, Tainan 70101, Taiwan*
[2]*Physics Division, National Center for Theoretical Sciences, Taipei 10617, Taiwan*

In this paper, we investigate the strong-coupling quantum thermodynamics of a hybrid quantum system far from equilibrium, based on the renormalization theory of quantum thermodynamics we developed recently [Phys. Rev. Research **4**, 023141 (2022)]. The strong-coupling hybrid system consists of a superconducting microwave cavity and a spin ensemble of the NV centers in diamond under external driving. The non-Markovian dynamics of this strong-coupling hybrid system has been experimentally explored and theoretically investigated. We apply the renormalization theory of quantum thermodynamics to study the transient quantum heat and work in this strong-coupling hybrid system. We find that the dissipation and fluctuation dynamics of the system induce the transient quantum heat current which shows significant non-Markovian effects. On the other hand, the energy and driving field renormalization produces quantum work power. In particular, the driving-induced work power can be largely enhanced by non-Markovian dynamics through the cavity coupling strongly with the spin ensemble at the resonance. Our results show that non-Markovian dynamics makes faster energy conversion of the heat and work.

I. INTRODUCTION

The investigation of quantum thermodynamics far from equilibrium has attracted great attention in the last decade [1–12], especially, the understanding of nonequilibrium energy conversion of heat and work in nanoscale devices is the key for building quantum heat engines. Incorporating with quantum features, nonequilibrium thermodynamics of nanoscale systems can exhibit exotic properties. For example, quantum coherence and entanglement could enhance the energy conversion efficiency of heat engines in comparison with classical counterparts [13–19]. It was also argued that quantum interference boosts the energy conversion efficiency in photosynthesis as a quantum engine [20–25]. However, these exotic quantum thermodynamics properties are usually extracted from the systems weakly coupled with their reservoirs. For the strong coupling between system and reservoir, the energy conversion of heat and work is not clearly understood. One of the main motivations in the study of quantum thermodynamics is to understand and manipulate energy conversion of heat and work in nanoscale and atomic-scale quantum systems when they strongly couple to their environment.

In fact, the definitions of thermodynamics quantities, such as heat and work, are quite ambiguous at quantum level. A contradiction has been pointed out in evaluating specific heat in strong-coupling system due to the different definition of internal energy [26,27]. In the previous investigations, the concept of heat and work has been focused on how to take into account properly the coupling energy between the system and its reservoir [28–33]. Even for a system operating at steady-state limit, the definition of heat and work is still debated within the framework of quantum mechanics [27,34–41]. For the system far from equilibrium, the transient processes of energy exchange become much more complicated in the strong coupling [42,43]. More detailed discussions can be found from the recent reviews [5–8]

In fact, the system-environment coupling will not only modify the system Hamiltonian, but also induce dissipation and fluctuations to the system dynamics at the same time. The renormalization of system Hamiltonian changes the energy spectrum distribution and interactions but does not change the unitary property of the system dynamics. The environment-induced dissipation and fluctuations make the system evolution nonunitary. It is the latter leads to the system thermalization [3,9] so that quantum thermodynamics can emerge. Furthermore, quantum mechanically, work is done by the system Hamiltonian renormalization, and heat arises from dissipation and fluctuations, as the consequence of entropy production. The lack of a consistent description of the system Hamiltonian renormalization together with dissipation and fluctuation for nonequilibrium evolution of open systems is perhaps the main problem faced in most of the previous investigations.

Very recently, we developed a renormalization theory of nonequilibrium quantum thermodynamics from the weak to strong couplings [12], based on the exact dynamics and thermalization of open quantum systems [44–49]. In this theory, the exact dynamics of open quantum systems is solved by nonperturbatively and exactly tracing over all reservoir states from the density matrix of the total system [44–49] through the coherent-state path integral [50]. Thus, all the

*Corresponding author: wzhang@mail.ncku.edu.tw

environmental effects on the system are taken into account without any ambiguity. Not only the renormalized system Hamiltonian, but also the dissipation and fluctuation dynamics naturally emerge together in the exact master equation of the reduced density matrix for the system. Consequently, we have provided rather unique definitions for various quantum thermodynamics quantities, including quantum heat and work [12]. In this paper, we shall extend the study to the transient energy conversion of heat and work in nonequilibrium quantum thermodynamics with an experimentally realized strong-coupling hybrid system in quantum optics.

The strong-coupling hybrid system is a superconducting microwave cavity interacted strongly with a spin ensemble made of NV centers in diamond. This system has been experimentally used to measure decoherence dynamics and quantum memory [51,52]. In particular, they measured how the decoherence dynamics is suppressed in the strong-coupling regime. The corresponding non-Markovian decoherence dynamics are analyzed in details [53,54], where theoretical solution also precisely reproduces the experiment results. Thus, it is interesting to see if this strong-coupling hybrid system controlled by external driving can serve as a quantum heat machine for studying energy conversion of heat and work quantum mechanically. We apply our exact description of non-Markovian decoherence dynamics [54] incorporating the theory of strong-coupling quantum thermodynamics [12] to this natural strong-coupling quantum system. We are also interested in providing a practically reliable physical system for further experimental measurement on non-Markovian quantum thermodynamics in the transient processes.

The non-Markovian dynamics, as a very important feature of open quantum systems, has been extensively studied in recent years. Most of the studies focus on the non-Markovianity with the concepts of divisibility or distinguishability, defined mathematically from completely positive and trace-preserving dynamical maps [55,56]. These dynamical maps lack the connection to the detailed spectral density of the open system. Physically, it is well known that the spectral density encapsulates all the effects of environment on the open system dynamics [57]. We have developed the general theory of non-Markovian dynamics in open quantum systems [58,59], where the general features of non-Markovian dynamics are determined by the spectral density. In this strong-coupling hybrid system, the spectral density has been experimentally fitted [51]. Therefore, it is particularly interesting to see how non-Markovian dynamics affects quantum thermodynamics, and how the heat and work transfers are influenced by non-Markovian dynamics. We find that the non-Markovian dynamics plays a significant role in the energy conversion of heat and work under the external driving. In a series of case studies, we also provide a direction for experimentalists to measure the transient heat and work in strong-coupling systems.

The rest of this paper is organized as follows. In Sec. II, we present a generalized Tavis-Cummings model for the hybrid system of a superconducting microwave cavity coupling strongly to the spin ensemble. The general nonequilibrium theory for such a strong-coupling system is reviewed and the features of non-Markivan dynamics and its physical meaning in transient transport processes are discussed. In Sec. III, we
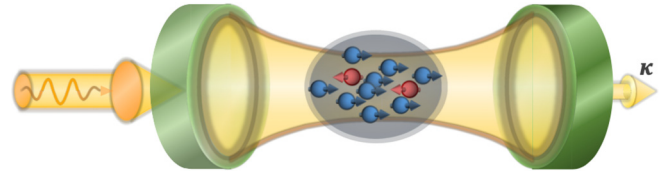
FIG. 1. A schematic diagram of the strong-coupling hybrid system consisting of a superconducting microwave cavity coupled with a spin ensemble of NV centers in diamond.

apply the quantum thermodynamics based on the nonequilibrium theory to study the transient quantum heat and work in the strong coupling. We find that the dissipation and fluctuation dynamics of the system induce quantum heat current which involves strong non-Markovian effects. On the other hand, the quantum work power arises from the renormalized energy and the renormalized driving field in the system Hamiltonian. Through the renormalization of the cavity energy and the driving field, the quantum work power is also affected significantly by non-Markovian dynamics. Experimental setup for the separate measurement of the quantum work power and heat current is also proposed. By tuning the driving and cavity frequency as well as the coupling strength between the cavity and spin ensemble, we show how non-Markovian dynamics is manifested in the energy conversion of heat and work in strong-coupling quantum thermodynamics. Finally, a conclusion is drawn in Sec. IV.

II. NONEQUILIBRIUM NON-MARKOVIAN THEORY OF THE STRONG-COUPLING HYBRID SYSTEM

The strong-coupling hybrid system concerned in this paper is investigated experimentally by Putz *et al.* [51,52]. It is a superconducting microwave cavity strongly coupled to a spin ensemble of the NV centers in diamond (see Fig. 1). Also, the cavity is driven by an external pulse so that one can manipulate and measure the nonequilibrium photon dynamics. Theoretically, the cavity photon dynamics can be well described by the generalized Tavis-Cummings model with the following Hamiltonian [60]:

$$H(t) = \hbar\omega_c a^\dagger a + [f(t)a^\dagger + \text{H.c.}]$$
$$+ \sum_i \hbar\Delta_i \sigma_i^z + \sum_k \hbar\omega_k b_k^\dagger b_k$$
$$+ \sum_i (V_i a^\dagger \sigma_i^- + V_i^* \sigma_i^+ a) + \sum_k (V_k a^\dagger b_k + V_k^* b_k^\dagger a).$$
$$(1)$$

Here, $a^\dagger$ (a) is the creation (annihilation) operator of cavity photon mode ω_c, and $f(t)$ is the external driving field applied to the cavity. The operators σ_i^z, $\sigma_i^\pm$ represent the three Pauli matrices of the ith spin in the spin ensemble with spin energy-level splitting $\hbar\Delta_i$. The parameter V_i is the coupling strength between the cavity mode and the ith spin of the spin ensemble. We also include the cavity leakage effects in Eq. (1) due to the weak coupling between the cavity and the free-space electromagnetic (EM) modes ω_k, where $b_l^\dagger$ (b_l) is the corresponding creation (annihilation) operator and V_k is the coupling strength between the cavity and EM modes.

In the practical experimental setup [51,52], spins of the NV centers in diamond are surrounded by Helmholtz coil which supplies a strong magnetic field to make all the spins into the polarized ground state. The total spin number is the order of 10^{12}. The external driving field applying to the cavity can excite about a small number of spins ($\approx 10^6$) [51,52]. This implies that the spin ensemble is a highly polarized spin ensemble. Thus, the Holstein-Primakoff approximation [61] $\sigma_i^+ \equiv c_i^\dagger (1 - c_i^\dagger c_i)^{-1/2} \simeq c_i^\dagger$, and $\sigma_i^z \equiv c_i^\dagger c_i - \frac{1}{2}$ can be applied to bosonalize the spin ensemble, where $c_i^\dagger$ (c_i) represents the bosonic creation (annihilation) operator of the corresponding ith spin. As a result, the Hamiltonian (1) can be reduced to

$$
\begin{aligned}
H(t) = {} & \hbar \omega_c a^\dagger a + [f(t)a^\dagger + \text{H.c.}] \\
& + \sum_i \hbar \Delta_i c_i^\dagger c_i + \sum_k \hbar \omega_k b_k^\dagger b_k \\
& + \sum_i (V_i a^\dagger c_i + V_i^* c_i^\dagger a) + \sum_k (V_k a^\dagger b_k + V_k^* b_k^\dagger a).
\end{aligned}
\tag{2}
$$

The nonequilibrium theory of this system has been formulated [46,54]. The cavity photon dynamics can be described by the cavity density matrix $\rho_c(t) = \text{Tr}_E[\rho_{tot}(t)]$. The total density matrix $\rho_{tot}(t)$ is determined from the Liouville–von Neumann equation of the total system (i.e., the cavity plus the spin ensemble and the free-space EM modes)

$$
i\hbar \frac{d}{dt} \rho_{\text{tot}}(t) = [H(t), \rho_{\text{tot}}(t)].
\tag{3}
$$

After tracing over all the environment degrees of freedom (including the spin ensemble and the free-space EM modes), we obtain the exact master equation of the cavity photonic state [46,54]

$$
\begin{aligned}
\frac{d}{dt} \rho_c(t) = {} & \frac{1}{i\hbar}\big[H_c^r(t, t_0), \rho_c(t)\big] \\
& + \gamma(t, t_0)[2a\rho_c(t)a^\dagger - a^\dagger a\rho_c(t) - \rho_c(t)a^\dagger a] \\
& + \tilde{\gamma}(t, t_0)[a\rho_c(t)a^\dagger + a^\dagger \rho_c(t)a - a^\dagger a\rho_c(t) \\
& - \rho_c(t)aa^\dagger].
\end{aligned}
\tag{4}
$$

Here, the first term describes the unitary evolution of the cavity density matrix with the renormalized system Hamiltonian

$$
H_c^r(t, t_0) = \hbar \omega_c^r(t, t_0)a^\dagger a + f_r^*(t, t_0)a + f_r(t, t_0)a^\dagger.
\tag{5}
$$

The renormalization is given by the renormalized frequency $\omega_c^r(t, t_0)$ and the renormalized driving field $f_r(t, t_0)$ arisen from the cavity coupling to the spin ensemble. The second and third terms in Eq. (4) give the nonunitary evolution of the cavity induced by the spin ensemble and also the leakage effect, which are characterized by the dissipation and fluctuation coefficients $\gamma(t, t_0)$ and $\tilde{\gamma}(t, t_0)$, respectively. They describe the cavity spontaneous emission into the spin ensemble (including the free-space leakage) and the induced cavity emission and absorption from the thermal fluctuations of the spin ensemble and the free space.

All the time-dependent parameters in the exact master equation (4), i.e., the renormalized frequency and the renormalized driving field, as well as the dissipation and fluctuation coefficients are nonperturbatively and exactly determined by the nonequilibrium Green functions [46]

$$
i\omega_c^r(t, t_0) + \gamma(t, t_0) = -\frac{\dot{u}(t, t_0)}{u(t, t_0)},
\tag{6a}
$$

$$
f_r(t, t_0) = i\hbar \dot{y}(t, t_0) - i\hbar \left[\frac{\dot{u}(t, t_0)}{u(t, t_0)} y(t, t_0)\right],
\tag{6b}
$$

$$
\tilde{\gamma}(t, t_0) = \dot{v}(t, t) - \left[\frac{\dot{u}(t, t_0)}{u(t, t_0)} v(t, t) + \text{c.c.}\right].
\tag{6c}
$$

The Green functions $u(t, t_0)$, $v(\tau, t)$ and the driving-induced cavity field $y(t, t_0)$ obey nonperturbatively the following time-convolution equations of motion:

$$
\begin{aligned}
& \frac{d}{dt} u(t, t_0) + i\omega_c u(t, t_0) + \int_{t_0}^{t} d\tau\, g(t, \tau)u(\tau, t_0) \\
& = 0,
\end{aligned}
\tag{7a}
$$

$$
\begin{aligned}
& \frac{d}{d\tau} v(\tau, t) + i\omega_c v(\tau, t) + \int_{t_0}^{\tau} d\tau'\, g(\tau, \tau')v(\tau', t) \\
& = \int_{t_0}^{t} dt'\, \tilde{g}(\tau, t')u^*(t, t') \quad (t_0 \leqslant \tau \leqslant t),
\end{aligned}
\tag{7b}
$$

$$
\begin{aligned}
& \frac{d}{dt} y(t, t_0) + i\omega_c y(t, t_0) + \int_{t_0}^{t} d\tau\, g(t, \tau)y(\tau, t_0) \\
& = \frac{1}{i\hbar} f(t),
\end{aligned}
\tag{7c}
$$

subjected to the initial condition $u(t_0, t_0) = 1$, $v(t_0, t) = 0$, and $y(t_0, t_0) = 0$. Because of the boundary conditions $v(t_0, t) = 0$ and $y(t_0, t_0) = 0$, Eqs. (7b) and (7c) can be analytically solved in terms of $u(t, t_0)$ [46]:

$$
v(\tau, t) = \int_{t_0}^{\tau} dt_1 \int_{t_0}^{t} dt_2\, u(\tau, t_1)\tilde{g}(t_1, t_2)u^*(t, t_2),
\tag{8a}
$$

$$
y(t, t_0) = \frac{1}{i\hbar} \int_{t_0}^{t} d\tau\, u(t, \tau)f(\tau).
\tag{8b}
$$

The integral kernels in the above time-convolution equations are given by the two-time system-environment correlation functions

$$
g(t, \tau) = \int_0^\infty \frac{d\omega}{2\pi} J(\omega)e^{-i\omega(t-\tau)},
\tag{9a}
$$

$$
\tilde{g}(t, \tau) = \int_0^\infty \frac{d\omega}{2\pi} J(\omega)\bar{n}(\omega, T)e^{-i\omega(t-\tau)}
\tag{9b}
$$

are the time-correlation functions between the cavity and the spin ensemble (also include the free space for the leakage). The spectrum density of the environment (spin ensemble plus the free space)

$$
\begin{aligned}
J(\omega) & = \frac{2\pi}{\hbar^2}\left[\sum_i |V_i|^2 \delta(\omega - \Delta_i/\hbar) + \sum_k |V_k|^2 \delta(\omega - \omega_k)\right] \\
& = J_s(\omega) + J_e(\omega)
\end{aligned}
\tag{10}
$$

represents the spectrum densities of the spin ensemble and the free-space EM field coupled with the cavity. The particle distribution $\bar{n}(\omega, T_0) = 1/(e^{\hbar \omega/k_B T_0} - 1)$ is the distribution of boson mode ω with temperature T_0 at the initial time t_0.

The non-Markovian memory due to the back-reaction between the cavity and environment is described by the time-convolution equations (7) and (8). It crucially depends the structure of spectral density. The spectrum density of the spin ensemble characterizes the inhomogeneous spectrum broadening due to the local magnetic dipole-dipole couplings between NV centers and the residual nitrogen paramagnetic impurities. It can be measured and manipulated in experiments [52]. It was found in the experiment [51] that the spectrum density of the spin ensemble $J_s(\omega)$ is a q-Gaussian spectrum, which is an intermediate form between a Gaussian spectral density ($q = 1$) and a Lorentzian spectral density ($q = 2$):

$$J_s(\omega) = 2\pi\Omega^2 C\left[1 - (1-q)\frac{(\omega - \omega_s)^2}{\Delta^2}\right]^{\frac{1}{1-q}}, \qquad (11)$$

where $q = 1.39$ is experimentally fitted, C is a normalization constant of the density of state, ω_s is the main frequency of the spin ensemble, Δ is determined by the full width at the half-maximum of $J_s(\omega)$ which is given by $d = 2\Delta\sqrt{\frac{2^{q-2}}{2q-2}}$, and the coupling strength is 2Ω. The free EM spectrum $J_e(\omega)$ is taken by the decay constant κ, describing the cavity leakage. Thus, $J(\omega) = J_s(\omega) + 2\kappa$.

In the experimental setup [51,52], the main frequency of spin ensemble is resonant with the cavity frequency $\omega_s = \omega_c = 2\pi \times 2.69$ GHz, the full width of the spin spectrum is fitted by $d = 18.8\pi$ MHz. Both the coupling strength and the temperature of the spin ensemble are experimentally adjustable. When the coupling strength is smaller than the half-width of the spectral density $2\Omega < d/2$, it is weak coupling and the cavity dynamics is Markovian. When $2\Omega > d/2$ which corresponds to the strong coupling and induces non-Markovian memory dynamics [54]. Specially, the stronger coupling induces the stronger non-Markovian dynamics that can suppress decoherence of the cavity field, as observed in experiment [51]. Theoretically, the decoherence suppression comes from the rapid oscillations between positive and negative values of the dissipation and fluctuation coefficients $\gamma(t, t_0)$ and $\tilde{\gamma}(t, t_0)$ in our exact master equation and determined by Eq. (6). Such rapidly transport oscillations keep energy and information (heat) flowing forth and back between the cavity and ensemble, as we will show in the next section. This is the physical picture of how strong non-Markovian dynamics can alter significantly the decoherence features [54].

It may be worth pointing out that in the literature, tremendous effects have been focused on the study of the so-called non-Markovianity based on divisibility and distinguishability arguments [55,56]. Both concepts come from the completely positive trace-preserving dynamical maps in open systems, which are mathematically defined for Markovian processes. Because these dynamical maps do not address the behaviors of non-Markovian processes, the physics of non-Markovian dynamics is often misinterpreted. In fact, the dynamics of open quantum systems is fully determined by their spectral densities with environments [57]. The non-Markovian dynamics is then controlled not only by the coupling strength, but also the profile of spectral density arisen from the environment spectral structure. This is shown in the theory of general non-Markovian dynamics we developed [58].

Specifically, consider the spectral density of Eq. (11). For the fixed spectral width $d = 2\Delta\sqrt{\frac{2^{q-2}}{2q-2}}$ which is determined from experiments, the strong or weak coupling ($2\Omega > d/2$ or $2\Omega < d/2$) results in the non-Markovian dynamics or Markovian dynamics, characterized by the time-dependent dissipation and fluctuation coefficients $\gamma(t, t_0)$ and $\tilde{\gamma}(t, t_0)$, which oscillate between the positive and negative values or oscillate with positive values all the time. The former describes the information (entropy or heat) and energy flowings forth and back between the system and environment that generates the memory, the latter makes the information and energy loss into the environment all the time so that no memory can be generated. Thus, non-Markovian dynamics is not simply given by oscillations. It is given by these transport oscillations in the dissipation and fluctuation processes that describe the flows of the energy and information forth and back between the system and environment [54,58]. All these transport phenomena crucially depend on the coupling strength and the profile of the spectral density. If the spectral width of the environment is very large (e.g., the white band limit) such that strong coupling does not make the height of the spectral density greater than the spectral width, the decoherence dynamics of open systems is always Markovian.

More precisely speaking, non-Markovian dynamics of an open system is a memory effect characterizing the correlation of event(s) at different times through the coupling to the surrounding environment. It is described by time-convolution equations of motion. The time-convolution kernels are the two-time system-environment correlation functions. For any open quantum system, if the dynamics is not described by time-convolution equation(s), it should not be able to describe non-Markovian dynamics. In our theory, the time-convolution equations are Eqs. (7), from which the open system dynamics is fully determined by the exact master equation (4) through various coefficients given in Eq. (6), including the the renormalized energy and driving field in the system Hamiltonian as well as the dissipation and fluctuation coefficients. This is a rigorous theory that encompasses all possible non-Markovian dynamics of open systems. Experimentally, measuring the two-time correlation functions is the direct physical observation of non-Markovian dynamics, as we also proposed [54,62].

Furthermore, as shown by Eqs. (6) and (7), the dissipation and fluctuation dynamics of open quantum systems are fully calculated from the nonequilibrium Green functions $u(t, t_0)$ and $v(t, t)$. Because these time-convolution equations of the nonequilibrium Green functions can be generalized to arbitrary interacting open quantum systems in quantum transport theory [63–65], our nonequilibrium non-Markovian theory can be applied to investigate non-Markovian dynamics for any open system, by simply calculating its nonequilibrium Green functions of the system in the standard many-body theory. It also recovers the quantum transport theory in many-body systems [45–47] so that nonequilibrium energy conversion of heat and work can be fully addressed. Specifically, the Green functions $u(t, t_0)$ and $v(t, t)$ correspond precisely to the retarded and correlation Green functions in nonequilibrium Green functions technique in many-body systems, as we have shown [45,46]. The retarded Green function $u(t, t_0)$

specifies the energy and driving field renormalization and the dissipation dynamics. The correlation Green function $v(t,t)$ of Eq. (8a) is the nonequilibrium generalization of the fluctuation-dissipation theorem [58], a theorem that any dynamics of open quantum systems must obey as a consequence of the unitary property of the total system. Hence, the system Hamiltonian renormalization and the dissipation and fluctuation dynamics are determined together from these nonequilibrium system Green functions, without the need to know the detailed reduced states of the system [58,59]. With such a general nonequilibrium theory, we are now able to explore the nonequilibrium quantum thermodynamics and energy conversion of heat and work in this hybrid system under the external driving field.

III. TRANSIENT QUANTUM WORK AND HEAT

A. General definition of quantum heat and quantum work

In the convention thermodynamics, the internal energy of a system is solely determined by the system Hamiltonian where it is assumed that the system interacts only very weakly with the reservoir. Beyond the weak-coupling regime, however, the internal energy must take into account system-environment coupling effect. In the literature, this is a difficult problem that has not been solved because it is not clear how much the coupling energy should be included in the system's Hamiltonian [26,27,30–32]. Based on our exact master equation, this difficult problem has been unambiguously overcome in our recent theory of renormalized quantum thermodynamics from weak to strong couplings [12]. In this renormalized quantum thermodynamics theory, the modification of the system Hamiltonian due to the strong system-reservoir coupling is given by the renormalization of the system Hamiltonian together with the dissipation and fluctuations, as shown in the exact master equation (4). The renormalized system Hamiltonian takes into account all possible energy renormalized effects arisen from the coupling to the reservoir, as did in the standard renormalization procedure in the many-body theory and in the quantum field theory [12,66,67]. The dissipation and fluctuation dynamics describes how the system is thermalized and thereby determine the energy conversion of the heat and work through transient transport nonequilibrium processes.

Explicitly, the internal energy $E^r(t)$ can be defined as the average of the renormalized cavity Hamiltonian in Eq. (4):

$$E^r(t) \equiv \langle H_c^r(t,t_0) \rangle = \text{Tr}_s[H_c^r(t,t_0)\rho_c(t)]$$
$$= \hbar\omega_c^r(t,t_0)\bar{n}(t) + 2\,\text{Re}[f_r^*(t,t_0)\langle a(t)\rangle], \quad (12a)$$

where

$$\bar{n}(t) = \text{Tr}_s[a^\dagger a\rho_c(t)] = |u(t,t_0)|^2\bar{n}(t_0) + |y(t,t_0)|^2$$
$$+ [u^*(t,t_0)\langle a^\dagger(t_0)\rangle y(t,t_0) + \text{c.c.}] + v(t,t) \quad (12b)$$

and

$$\langle a(t)\rangle = \text{Tr}_s[a\rho_c(t)] = u(t,t_0)\langle a(t_0)\rangle + y(t,t_0). \quad (12c)$$

The notation Tr_s denotes the trace over the cavity states, and $\omega_c^r(t,t_0)$ is the renormalized cavity frequency determined by Eq. (6a). The average photon number $\bar{n}(t)$ describes the

cavity field intensity which is related to the initial cavity field and the initial cavity occupation number, $\langle a^\dagger(t_0)\rangle$ and $\bar{n}(t_0)$, and the driving-induced cavity field $y(t,t_0)$. The nonequilibrium Green functions $u(t,t_0)$, $v(t,t)$, and $y(t,t_0)$ are determined by the time-convolution equations (7) and (8), from which the non-Markovian dynamics is precisely described.

Thermodynamically, energy can enter into or leave from a system through heat and work. Heat is arisen from the change of the entropy in state populations. Quantum mechanically, work corresponds to the changes in energy levels of the system and also the driving field. Accordingly, we can introduce the quantum work power and quantum heat current as follows [12]:

$$\mathcal{P}_w(t) \equiv \text{Tr}_s\left[\frac{dH_c^r(t,t_0)}{dt}\rho_c(t)\right], \quad (13a)$$

$$\mathcal{I}_h(t) \equiv \text{Tr}_s\left[H_c^r(t,t_0)\frac{d\rho_c(t)}{dt}\right]. \quad (13b)$$

Based on the exact master equation (4), the above transient work power and the heat current can be expressed explicitly as

$$\mathcal{P}_w(t) = \bar{n}(t)\frac{d}{dt}\left[\hbar\omega_c^r(t,t_0)\right] + 2\,\text{Re}\left[\langle a(t)\rangle\frac{df_r^*(t,t_0)}{dt}\right], \quad (14a)$$

$$\mathcal{I}_h(t) = \hbar\omega_c^r(t,t_0)\tilde{\gamma}(t,t_0) - 2\gamma(t,t_0)[E^r(t)$$
$$- \text{Re}[\langle a(t)\rangle f_r^*(t,t_0)]]. \quad (14b)$$

In the weak coupling, if one ignores the energy and the driving field renormalization, and also takes simply the dissipation as a constant decay rate and ignores the thermal fluctuations, can can easily reproduce the results introduced early by Alicki based on the Markov master equation for the weak coupling [28].

In Eq. (14a), the quantum work power consists of two contributions, the intrinsic contribution arisen from the energy renormalization and the extrinsic contribution generated from the renormalization of driving field, denoted, respectively, by

$$\mathcal{P}_w^e = \bar{n}(t)d\left[\hbar\omega_c^r(t,t_0)\right]/dt, \quad (15a)$$

$$\mathcal{P}_w^d(t) = 2\,\text{Re}[\langle a(t)\rangle df_r^*(t,t_0)/dt]. \quad (15b)$$

As the system interacts with its environment, the system and the environment do the work on each other through the shift of their energy levels. In addition, the extrinsic work is given by the driving-induced work power where the renormalization of the driving field coming from the back-action from the spin ensemble. Thus, the non-Markovian cavity dynamics also changes significantly the driving-induced work power through Eqs. (6b) and (7b).

On the other hand, the quantum heat current in Eq. (14b) also consists of two contributions: $\hbar\omega_c^r(t,t_0)\tilde{\gamma}(t,t_0)$ and $-2\gamma(t,t_0)[E^r(t) - \text{Re}[\langle a(t)\rangle f_r^*(t,t_0)]]$. They are proportional to the fluctuation coefficient $\tilde{\gamma}(t,t_0)$ and the dissipation coefficient $\gamma(t,t_0)$, respectively [see Eqs. (4) and (6)]. It shows that quantum heat is induced not only from fluctuations, but also from dissipation dynamics. The internal energy consists of the driving and initial-cavity-state related energy

as well as the energy arisen from thermal fluctuations, as shown in Eq. (12) in which $v(t, t)$ is the thermal fluctuation correlation. Thus, we can define, respectively, the fluctuation heat current $\mathcal{I}_h^{\mathcal{F}}(t)$ and the dissipation heat current $\mathcal{I}_h^{\mathcal{D}}(t)$ as follows:

$$\mathcal{I}_h^{\mathcal{F}}(t) = \hbar\omega_c^r(t, t_0)[\tilde{\gamma}(t, t_0) - 2\gamma(t, t_0)v(t, t)]$$
$$= \hbar\omega_c^r(t, t_0)\dot{v}(t, t), \tag{16a}$$

$$\mathcal{I}_h^{\mathcal{D}}(t) = -2\gamma(t, t_0)[E^r(t)|_{T=0} - \text{Re}[\langle a(t)\rangle f_r^*(t, t_0)]], \tag{16b}$$

where

$$E^r(t)|_{T=0} = \hbar\omega_c^r(t, t_0)[|u(t, t_0)|^2\bar{n}(t_0) + |y(t, t_0)|^2$$
$$+ [u^*(t, t_0)\langle a^\dagger(t_0)\rangle y(t, t_0) + \text{c.c.}]] \tag{16c}$$

is obtained from Eq. (12). It is the part of the internal energy that depends on the initial cavity state and the driving field but independent of the thermal fluctuations. As one can see, the fluctuation heat current $\mathcal{I}_h^{\mathcal{F}}(t)$ is fully determined by the thermal fluctuation correlation $v(t, t)$. The dissipation heat current $\mathcal{I}_h^{\mathcal{D}}(t)$ is governed by various dissipation processes. The above formulation for the energy conversion of work and heat is valid for both the weak and strong couplings.

Moreover, the transient work power and heat current given above can be measured separately in experiments. As shown in the previous experiments [51,52], the cavity frequency ω_c and the temperature of the spin ensemble are adjustable, the coupling strength Ω in Eq. (11) can be taken from a few MHz to a few tens MHz (from the weak to strong couplings), and the driving field can be turned on and off. Thus, one can measure work power and heat current separately as follows:

(1) Measure the fluctuation heat current $\mathcal{I}_h^{\mathcal{F}}(t)$: Because the experimentally fitted spectral density $J_s(\omega)$ is a symmetric function with respect to the main spin frequency ω_s, as shown by Eq. (11), the cavity frequency shift is zero (no energy renormalization) if one sets $\omega_s = \omega_c$ (this setup was done in the experiment [51]). Thus, $\omega_c^r(t, t_0) = \omega_c$ (as one can also see the numerical calculation given in the next section). Meantime, turning the driving field off, $f(t) = 0$, so that $y(t, t_0) = 0$ and $f_r(t, t_0) = 0$. Then, no work power can be produced, i.e., $\mathcal{P}_w(t) = 0$ [see Eq. (14a)]. Let the cavity initially be in vacuum, i.e., $\bar{n}(t_0) = 0$ and $\langle a^\dagger(t_0)\rangle = 0$. The energy change one can measure only comes from the heat current induced by thermal fluctuation, given by $\mathcal{I}_h^{\mathcal{F}}(t) = \hbar\omega_c\dot{v}(t, t)$.

(2) Measure the dissipation heat current $\mathcal{I}_h^{\mathcal{D}}(t)$: With the same condition as given in step 1 but let the cavity initially not be empty [i.e., $\bar{n}(t_0) \neq 0$], then the energy change one measured is given by the total heat current $\mathcal{I}_h(t) = \hbar\omega_c[\dot{v}(t, t) - 2\gamma(t, t_0)|u(t, t_0)|^2\bar{n}(t_0)]$. Subtracting the fluctuation heat current $\mathcal{I}_h^{\mathcal{F}}(t)$ measured in step 1 from $\mathcal{I}_h(t)$, one can find the heat current purely induced by the cavity dissipation $\mathcal{I}_h^{\mathcal{D}}(t) = -2\gamma(t, t_0)|u(t, t_0)|^2\bar{n}(t_0)$. Or, alternatively, one can cool down the spin ensemble to very low temperature such that $v(t, t) \to 0$ which was indeed done in experiments [51,52] (also see our previous theoretical calculation [54]). Then, the energy change measured is only the dissipation heat current $\mathcal{I}_h^{\mathcal{D}}(t)$.

(3) Measure the renormalized work power $\mathcal{P}_w^e(t)$: Now turn the cavity frequency ω_c away from the main frequency

of the spin ensemble ω_s, i.e., let $\omega_c \neq \omega_s$, then cavity-spin ensemble coupling induces the cavity frequency shift: $\omega_c \to \omega_c^r(t, t_0)$. Meantime, keep the spin ensemble in very low temperature $v(t, t) \to 0$. The energy change one measured is given by $\bar{n}(t)\frac{d}{dt}[\hbar\omega_c^r(t, t_0)] - 2\gamma(t)\hbar\omega_c^r(t, t_0)|u(t, t_0)|^2\bar{n}(t_0) = \mathcal{P}_w^e(t) + \mathcal{I}_h^{\mathcal{D}}(t)$. Substracting the dissipation heat current $\mathcal{I}_h^{\mathcal{D}}(t)$ measured in step 2, one can find the renormalized work power $\mathcal{P}_w^e(t)$ induced by the the cavity-spin ensemble coupling.

(4) Measure the driving-induced work power $\mathcal{P}_w^d(t)$: Now, turning the driving field on, but keep the cavity initially in vacuum state and the spin ensemble in very low temperature with $\omega_c = \omega_s$, then we have $\langle a(t)\rangle = y(t, t_0)$ and $\bar{n}(t) \simeq |y(t, t_0)|^2$. One can measure the average cavity photon number or the cavity field amplitude $y(t, t_0)$, which can be used to determine the renormalized driving field $f_r(t, t_0)$. Then, one can find the driving-induced work power and the dissipation heat current from the following relations:

$$\mathcal{P}_w(t) = \mathcal{P}_w^d(t) = 2\,\text{Re}[y(t, t_0)df_r^*(t, t_0)/dt], \tag{17a}$$

$$\mathcal{I}_h(t) = \mathcal{I}_h^{\mathcal{D}}(t) = -2\gamma(t, t_0)[\hbar\omega_c|y(t, t_0)|^2$$
$$- \text{Re}[y(t, t_0)f_r^*(t, t_0)]]. \tag{17b}$$

With such solutions extracted from experiments, one can also determine the efficiency of this strong-coupling hybrid system under the driving, as a quantum heat machine.

Now, we can investigate the transient energy exchange in this strong-coupling hybrid system.

B. Transient quantum work and heat at strong coupling

We consider first a simple situation of the cavity being initially in a coherent state $|z_0\rangle$ and decoupled with the reservoir [$J(\omega) = 0$] to understand the pure driving dynamics. For simplicity, we also set the initial time $t_0 = 0$. The cavity is driven by an external time-dependent field $f(t) = Ae^{-i\omega_d t}$ with the constant amplitude A and the frequency ω_d. In this trivial case, we obtain the free Green function $u(t, \tau) = e^{-i\omega_c(t-\tau)}$ from Eq. (7) for the cavity. There is no energy renormalization to the system because the cavity is decoupled from the reservoir. Also, the driving field $f_r(t) = f(t)$ remains unchanged. The cavity photon state evolves into a coherent state $|\psi(t)\rangle = \exp\{z(t)a^\dagger + z^*(t)a\}|0\rangle$ where $z(t) = [z_0 + \frac{A}{\hbar\delta}(1 - e^{i\delta t})]e^{-i\omega_c t}$ is the field amplitude and $\delta = \omega_c - \omega_d$ is the detuning. From these results, we obtain the internal energy of the cavity and the cavity work power driving by the external field

$$E(t) = \langle H_c\rangle(t)$$
$$= \hbar\omega_c|z_0|^2 + 2\,\text{Re}\left[\frac{A^*z_0}{\delta}(w_c - w_d e^{-i\delta t})\right]$$
$$+ \frac{2|A|^2}{\hbar\delta^2}\omega_d[1 - \cos(\delta t)], \tag{18a}$$

$$\mathcal{P}_w(t) = 2\,\text{Re}\left[z(t)\frac{df^*(t)}{dt}\right]$$
$$= \frac{2|A|^2}{\hbar\delta}\omega_d\sin(\delta t) - 2\,\text{Im}[A^*z_0e^{-i\delta t}]w_d, \tag{18b}$$

$$\mathcal{I}_h(t) = 0. \tag{18c}$$
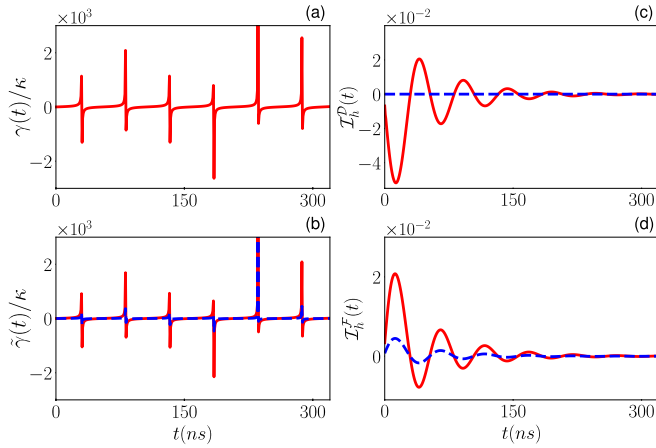
FIG. 2. The cavity is strongly coupled to the spin ensemble with main frequency $\omega_s = \omega_c$. (a) The dissipation coefficient $\gamma(t)$, (b) the fluctuation coefficient $\tilde{\gamma}(t)$, (c) the dissipation heat current $\mathcal{I}_h^{\mathcal{D}}(t)$, and (d) the fluctuation heat current $\mathcal{I}_h^{\mathcal{F}}(t)$ are plotted as a function of time. In (c) and (d), the units are $\hbar\omega_c/ns$. The system is initially prepared in a vacuum state $|0\rangle$ and a coherent state $|z_0\rangle$ with $z_0 = 1$ [corresponding to the blue dashed line and the red solid line in (c), respectively]. Also, the temperature $T_0 = 0.05$ and 0.1 K [corresponding, respectively, to the blue dashed lines and the red solid lines in (b) and (d)]. We also take the coupling strength $\Omega = 17.2\pi$ MHz (strong coupling), and the decay constant $\kappa = 0.8\pi$ MHz. No driving is applied in this case.

Of course, there is no heat production in an isolated system as one expected. By tuning the driving field frequency, we can control the power dynamics and drive the cavity system cyclically as an ideal optical engine. Furthermore, Eq. (18) is reduced to $E(t) = \hbar\omega_c|z_0|^2 + \frac{|A|^2}{\hbar}\omega_c t^2$, $\mathcal{P}_w(t) = \frac{2|A|^2}{\hbar}\omega_c t$ if we tune the driving field to the resonance and in phase with the system, i.e., $\delta = 0$ and $\text{Im}[A^*z_0] = 0$. Thus, the cavity behaves as an ideal optical resonator.

1. Quantum work power and the quantum heat currents

We now return to the hybrid cavity system. We first consider that the spin ensemble is at a finite temperature T_0, and meantime we also turn off the driving. Because the spectrum density of the spin ensemble is a symmetric function with respect to the main spin frequency ω_s [see Eq. (11)], if we turn the cavity frequency ω_c to resonant with the main frequency of the spin ensemble, i.e., let $\omega_s = \omega_c$, we find that there is no cavity frequency shift by the cavity-spin coupling due to the symmetric property of the spectral density. In this case, there is no energy renormalization so that the quantum work is zero. As a result, the changes of internal energy are caused only by the dissipation heat and the fluctuation heat, i.e., $dE^r(t)/dt = \mathcal{I}_h^{\mathcal{D}}(t) + \mathcal{I}_h^{\mathcal{F}}(t)$ in the nonequilibrium evolution.

In Fig. 2, we show the dissipation coefficient $\gamma(t)$ and the fluctuation coefficient $\tilde{\gamma}(t)$ in the left panel and plot the dissipation heat current $\mathcal{I}_h^{\mathcal{D}}(t)$ and the fluctuation heat current $\mathcal{I}_h^{\mathcal{F}}(t)$ in the right panel as a function of time. In the strong coupling, $2\Omega = 34.4\pi$ MHz $> d/2 = 9.4\pi$ MHz used in the experiment [51]. The dissipation and fluctuation coefficients show oscillations between positive and negative values with the spiky amplitudes [see Figs. 2(a) and 2(b)]. These spiky
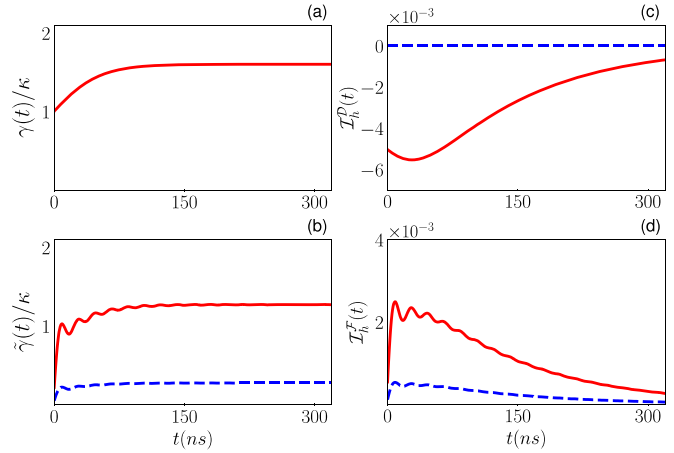
FIG. 3. The cavity is weakly coupled to the spin ensemble with main frequency $\omega_s = \omega_c$. (a) The dissipation coefficient $\gamma(t)$, (b) the fluctuation coefficient $\tilde{\gamma}(t)$, (c) the dissipation heat current $\mathcal{I}_h^{\mathcal{D}}(t)$, and (d) the fluctuation heat current $\mathcal{I}_h^{\mathcal{F}}(t)$ are plotted as a function of time. The coupling strength Ω is 1.72π MHz (weak coupling). Other parameters and units are the same as in Fig. 2

features characterize indeed the strongest non-Markovian dynamics in the strong coupling, as we have observed previously [54,68]. It indicates how the system and the environment rapidly exchange information and energy each other, as the memory effect. Such rapid oscillations accompany system information and energy fast flowing into and out of the spin ensemble, describing entropy production, the source of heat as a non-Markovian effect. In quantum thermodynamics, the non-Markovian dynamics leads to entropy production that generates heat currents flows forth and back between the cavity and the spin ensemble, as demonstrated in Figs. 2(c) and 2(d). Figures 2(c) and 2(d) also show that the dissipation heat current is always out of phase with the fluctuation heat current. This out-of-phase phenomenon indicates that the dissipation and fluctuation dynamics both bring the energy and fluctuation flows back and forth between the system and environment, will eventually make the system and environment approach to thermal equilibrium. It also shows explicitly that if the initial cavity is empty, one can measure the fluctuation heat current alone. On the other hand, making the spin ensemble initially in a very low temperature, the dissipation heat current dominates the heat flowing.

As a comparison, we also present the results in the weak coupling $2\Omega = 3.44\pi$ MHz $< d/2$ (see Fig. 3). In contrast to the strong coupling, the dissipation and fluctuation coefficients in Figs. 3(a) and 3(b) monotonically approach to a steady value, i.e., no oscillation between positive and negative values. In other words, there are no transport oscillations of the work and heat flowing forth and back between the system and environment. As a result, the dissipation heat current is always negative, carrying energy and information left away from the system, as shown by Figs. 3(c) and 3(d). However, the fluctuation heat current is always positive, namely, it brings energy and information from the environment back into the system. These single-direction energy and information transfers are typical Markovian processes in the weak coupling.
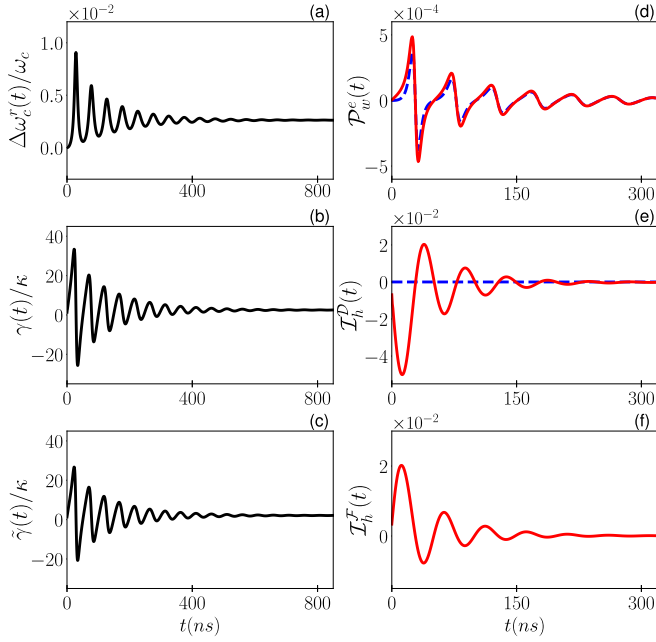
FIG. 4. The cavity is strongly coupled to the spin ensemble with main frequency $\omega_s = 0.998\omega_c$. (a) The renormalized frequency $\Delta\omega_c^r(t) = \omega_c^r(t) - \omega_c$, (b) the dissipation coefficient $\gamma(t)$, (c) the fluctuation coefficient $\tilde{\gamma}(t)$, (d) the quantum work power $\mathcal{P}_\omega^e(t)$, (e) the dissipation heat current $\mathcal{I}_h^{\mathcal{D}}(t)$, and (f) the fluctuation heat current $\mathcal{I}_h^{\mathcal{F}}(t)$ are plotted as a function of time. In (d)–(f), the units are $\hbar\omega_c/ns$. The system is initially prepared in a coherent state $|z_0\rangle$ with $z_0 = 0$ and 1 [corresponding to the blue dashed line and the red solid line in (c) and (d), respectively; other quantities are independent of the cavity initial state]. Other parameters are the strong-coupling strength $\Omega = 17.2\pi$ MHz, the decay constant $\kappa = 0.8\pi$ MHz, and the temperature $T = 0.1$ K.

To show a more complete picture of energy and information exchange between the system and environment, we next discuss the nonresonance case $\omega_s \neq \omega_c$ in Eq. (11). In the nonresonance case, the energy renormalization occurs. In the left panel of Fig. 4, we show the renormalized frequency $\omega_c^r(t)$, the dissipation coefficient $\gamma(t)$, the fluctuation coefficient $\tilde{\gamma}(t)$, and in the right panel, it shows the quantum work power $\mathcal{P}_w^e(t)$, the dissipation heat current $\mathcal{I}_h^{\mathcal{D}}(t)$, and the fluctuation heat current $\mathcal{I}_h^{\mathcal{F}}(t)$, respectively. We can see that, in addition to heat, intrinsic quantum work also contributes to the change of the internal energy, i.e., $dE^r(t)/dt = \mathcal{P}_w^e(t) + \mathcal{I}_h^{\mathcal{D}}(t) + \mathcal{I}_h^{\mathcal{F}}(t)$. As shown by Figs. 4(b) and 4(c), non-Markovian oscillations between positive and negative values for the dissipation and fluctuation coefficients are still significant for the nonresonance case, but the effect is weakened in comparing with the resonance case with the spiky features shown in Figs. 2(a) and 4(b). The oscillation amplitudes of dissipation and fluctuations show that the exchange of energy and information is not as dramatic as in the resonance case but is still significantly observable. Despite this, the behavior of heat currents is similar for both the resonance and nonresonance cases. Furthermore, the magnitudes of the quantum work power is very small. In other words, the dissipation effect $\gamma(t)$ and the fluctuation effect $\tilde{\gamma}(t)$ are much stronger than the energy renormalization in this hybrid system.
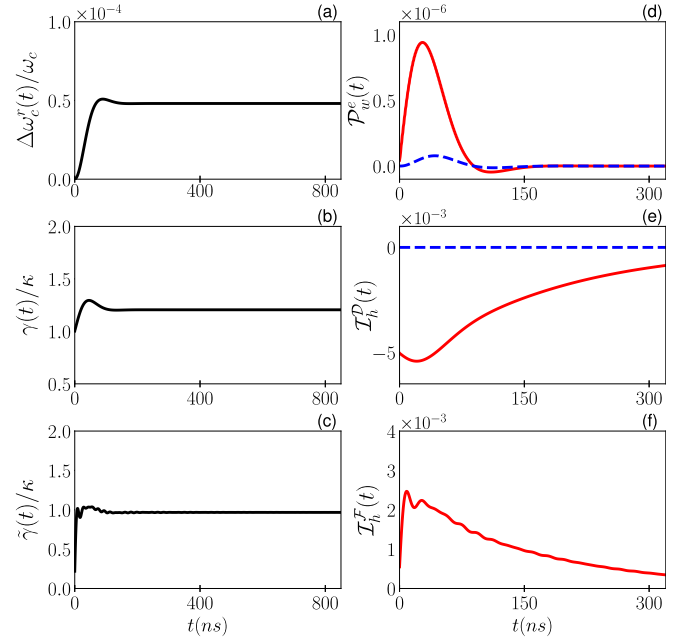
FIG. 5. The cavity is weakly coupled to the spin ensemble with main frequency $\omega_s = 0.998\omega_c$. (a) The renormalized frequency $\Delta\omega_c^r(t) = \omega_c^r(t) - \omega_c$, (b) the dissipation coefficient $\gamma(t)$, (c) the fluctuation coefficient $\tilde{\gamma}(t)$, (d) the quantum work power $\mathcal{P}_\omega^e(t)$, (e) the dissipation heat current $\mathcal{I}_h^{\mathcal{D}}(t)$, and (f) the fluctuation heat current $\mathcal{I}_h^{\mathcal{F}}(t)$ are plotted as a function of time. The coupling strength Ω is 1.72π MHz. Other parameters and units are the same as in Fig. 4.

let the cavity initially be in vacuum state, the dissipation heat current vanishes and the fluctuation heat current is the same as that in the resonance case (no energy renormalization) [see Fig. 2(d)]. Thus, by measuring the total energy changes, one can extract the renormalized energy-induced work power, even though it is a small effect.

To compare the results in strong coupling for the non-resonance case, we present the corresponding results for the weak coupling in Fig. 5. As one can see, the dissipation and fluctuation coefficients in Figs. 5(a)–5(c) have positive values all the time so that the cavity dynamics is Markovian, even though the energy has been renormalized. Comparing Figs. 4(a) and 4(d) with Figs. 5(a) and 5(d), the energy renormalization and the quantum work power both are smaller by two orders of magnitude for the weak coupling. In other words, the environment-induced thermodynamical effects are negligible in the weak coupling, as one expected. As a summary of the results presented in Figs. 2–5, we show how the non-Markovian dissipation and the fluctuation dynamics dominate the heat current transfer. In the strong coupling, both energy and heat flow forth and back rapidly between the system and the environment, manifesting the significance of non-Markovian dynamics in the strong-coupling quantum thermodynamics.

2. Transient energy exchanges due to non-Markovian dynamics

Next, we consider the transient thermodynamics under driving. The system is prepared in a vacuum state and applied by an oscillating driving field $f(t) = f_m e^{-i\omega_c t}\theta(t - t_s)$, where
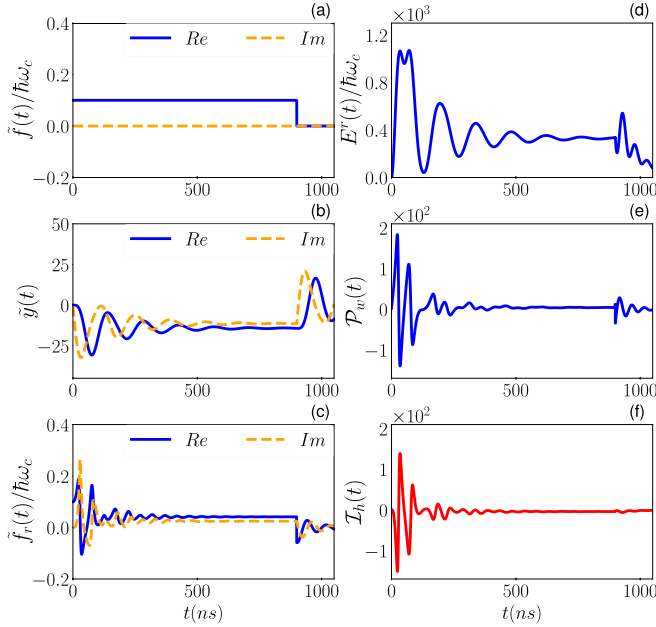
FIG. 6. A driving $f(t) = f_m e^{-i\omega_c t}\theta(t - t_s)$ is applied to the cavity which is strongly coupled to the spin ensemble with main frequency $\omega_s = 0.998\omega_c$. (a) The driving amplitude $\tilde{f}(t) = f(t)e^{i\omega_c t}$, (b) the induced cavity field amplitude $\tilde{y}(t) = y(t)e^{i\omega_c t}$, (c) the renormalized field amplitude $\tilde{f}_r(t) = f_r(t)e^{i\omega_c t}$, where $y(t)$ and $f_r(t)$ are determined by Eqs. (6b) and (7b), (d) the internal energy $E^r(t)$, (e) the quantum work power $\mathcal{P}_w(t)$ (blue solid line), and (f) the quantum heat current $\mathcal{I}_h(t)$ (red dashed line) are plotted as a function of time. In (a)–(c), the blue solid and orange dashed lines correspond to the real and the image part, respectively. The units in (d)–(f) are $\hbar\omega_c/ns$. The system is initially prepared in the vacuum state $|0\rangle$. Other parameters are the driving amplitude $f_m = \hbar\omega_c/10$, the turn off time $t_s = 900$ (ns), the coupling strength $\Omega = 17.2\pi$ MHz, the decay constant $\kappa = 0.8\pi$ MHz, and the temperature $T_0 = 0.1$ K.

ω_c is the cavity photon frequency and $\theta(t - t_s)$ means that the driving is applied only in the time interval $t_0 \rightarrow t_s$. After t_s, the driving is turned off. Because the renormalization of energy is very weak as shown in Fig. 4, the total quantum work power is dominated by the driving. On the other hand, the fluctuation heat current $\mathcal{I}_h^{\mathcal{F}}(t)$ does not depend on the driving field. It can be suppressed by lowering the spin-ensemble temperature, as shown in Fig. 2(d). That is, the total energy change is mainly determined by $dE^r(t)/dt \approx \mathcal{P}_w^d(t) + \mathcal{I}_h^D(t)$. In Figs. 6(a)–6(f), we show the driving field amplitude $\tilde{f}(t)$, the driving induced cavity field amplitude $\tilde{y}(t)$, the renormalized driving field amplitude $\tilde{f}_r(t)$ as a feedback of the cavity coupling with the spin ensemble, and also the internal energy of the cavity $E^r(t)$, the work power $\mathcal{P}_w(t)$, and the heat current $\mathcal{I}_h(t)$, The latter three thermodynamic quantities are controllable by the driving.

Applying the driving $f(t)$ as shown Fig. 6(a), all quantities exhibit oscillations in the beginning [see Figs. 6(b)–6(d). As we have discussed in general on non-Markovian dynamics, the oscillations in the renormalized driving field $f_r(t)$, the heat current and the work power manifest the strong non-Markovian dynamics. The oscillations of the renormalized driving, work power, and heat current between positive and
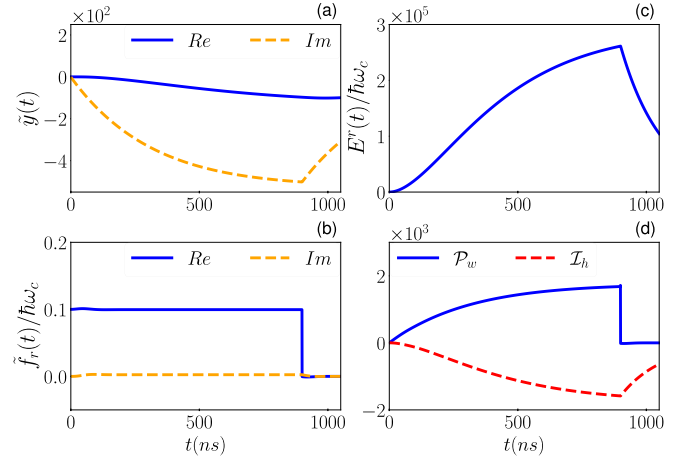
FIG. 7. A driving $f(t) = f_m e^{-i\omega_c t}\theta(t - t_s)$ is applied to the cavity which is weakly coupled to the spin ensemble with main frequency $\omega_s = 0.998\omega_c$. (a) The induced cavity field amplitude $\tilde{y}(t) = y(t)e^{i\omega_c t}$, (b) the renormalized field amplitude $\tilde{f}_r(t) = f_r(t)e^{i\omega_c t}$, (c) the internal energy $E^r(t)$, (d) the quantum work power $\mathcal{P}_w(t)$ (blue solid line) and the quantum heat current $\mathcal{I}_h(t)$ (red dashed line) are plotted as a function of time. The coupling strength $\Omega = 1.72\pi$ MHz. Other parameters and units are the same as in Fig. 6.

negative values describe the energy, work, and heat (information) flowing forth and back between the cavity and the spin ensemble, as shown in Figs. 6(c), 6(e), and 6(f). On the other hand, the cavity field $y(t)$ and the internal energy $E^r(t)$ also oscillate but these two quantities represent effectively the cavity field amplitude and the cavity field intensity. They do not directly describe the transport so that the oscillations behave different from that of the renormalized driving, the work power, and the heat current. But, these oscillations do arise from the non-Markovian dynamics through the renormalized driving, the work power, and the heat current.

Due to the non-Markovian decoherence, all physical quantities reach the steady values after a certain time, as a consequence of the balance between the external driving energy and the dissipation of the cavity and the fluctuations of the spin ensemble. In the steady state, the magnitudes of the renormalized driving, the work power, and the heat current approach almost to zero, which seems to make the system not so useful as a heat machine. When the driving is turned off at $t = t_s$, the steady cavity state will decay again and meantime the spin-ensemble energy retrieves back to the cavity. It still shows the non-Markovian oscillations after t_s, as shown in Figs. 6(b) and 6(d), but the magnitude is much smaller without the original driving.

As a comparison, we show the corresponding results in the weak-coupling regime in Fig. 7. Because of the Markovian dynamics in the weak coupling, in contrast to Fig. 6, there is no signal to show the energy transfer forth and back between the cavity and the spin ensemble, as shown in Fig. 7. Because we apply the same driving field, it shows that the oscillations in Fig. 6 are purely induced by non-Markovian dynamics. Furthermore, comparing the result of Fig. 7(b) with Fig. 6(a), one can see the renormalized driving field is almost the same as the original driving field. In other words, the renormalization effect is negligible in the driving field in the weak coupling.
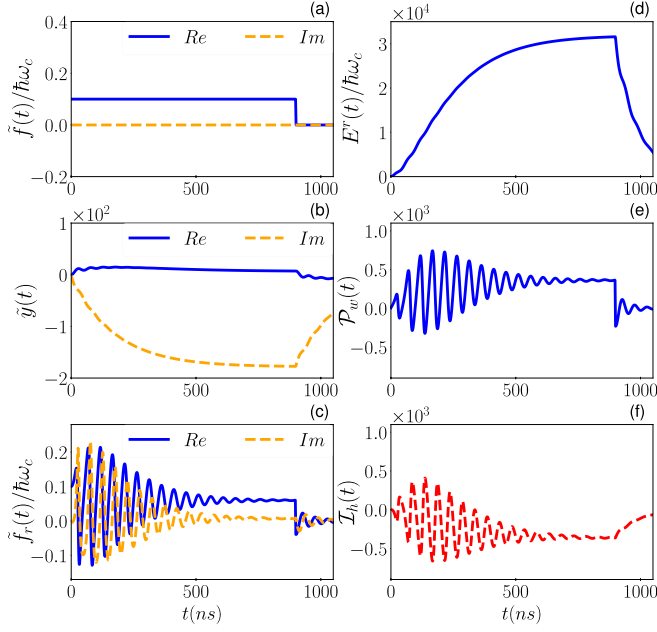
FIG. 8. A driving $f(t) = f_m e^{-i\omega_c^r t}\theta(t - t_s)$ is applied to the cavity which is strongly coupled to the spin ensemble with main frequency $\omega_s = 0.998\omega_c$. (a) The driving $\tilde{f}(t) = f(t)e^{i\omega_c^r t}$, (b) the induced cavity field $\tilde{y}(t) = y(t)e^{i\omega_c^r t}$, (c) the renormalized field $\tilde{f}_r(t) = f_r(t)e^{i\omega_c^r t}$, where $y(t)$ and $f_r(t)$ are determined by Eqs. (6b) and (7b), (d) the internal energy $E^r(t)$, (e) the quantum work power $\mathcal{P}_w(t)$, and (f) the quantum heat current $\mathcal{I}_h(t)$ are plotted as a function of time. Other parameters and units are the same as in Fig. 6.

FIG. 9. A driving $f(t) = f_m e^{-i\omega_c t}\theta(t - t_s)$ is applied to the cavity which is strongly coupled to the spin ensemble with main frequency $\omega_s = \omega_c$. (a) The driving $\tilde{f}(t) = f(t)e^{i\omega_c t}$, (b) the induced cavity field $\tilde{y}(t) = y(t)e^{i\omega_c t}$, (c) the renormalized field $\tilde{f}_r(t) = f_r(t)e^{i\omega_c t}$, where $y(t)$ and $f_r(t)$ are determined by Eqs. (6b) and (7b), (d) the internal energy $E^r(t)$, (e) the quantum work power $\mathcal{P}_w(t)$, and (f) the quantum heat current $\mathcal{I}_h(t)$ are plotted as a function of time. Other parameters and units are the same as in Fig. 6.

Furthermore, the results in Figs. 6(e) and 7(d) show that the driving-induced work power is stronger in the weak coupling. This is because the dissipation is very weak in the weak coupling. This indicates that the enhancement of dissipation reduces the driving-induced work power. As a result, the work power in the strong-coupling system is lowered down, even for the same driving source.

To get a more complete picture for the difference between the strong and weak couplings, we consider the system with a resonant driving field, i.e., modulating the driving field frequency to match the steady value of the renormalized frequency $\omega_c^r(t)$. In Fig. 8, we show the driving field amplitude $\tilde{f}(t)$, the cavity field amplitude $\tilde{y}(t)$, the renormalized driving field amplitude $\tilde{f}_r(t)$, the internal energy $E^r(t)$, the work power $\mathcal{P}_w(t)$, and the heat current $\mathcal{I}_h(t)$ in the strong coupling. Similar to Figs. 6(c), 6(e), and 6(f), the results in Figs. 8(c), 8(e), and 8(f) show that the renormalized driving field, the work power, and the heat current influenced by the stronger non-Markovian oscillations with a longer oscillating time and much larger amplitudes. In other words, the resonance between the driving field and the renormalized cavity frequency significantly enhances the non-Markovian dynamics. As a result, the steady-state renormalized driving field in the resonance case is only slightly smaller than the original driving field, in comparing with the nonresonance one, where the renormalized driving field almost vanishes as shown in Fig. 6(c). Meanwhile, the magnitudes of heat current and work power in the steady state [see Figs. 8(e) and 8(f)] are almost three orders of magnitudes larger than that in the nonresonant

case [see Figs. 6(e) and 6(f)]. This is a very remarkable result: it indicates that making the driving field resonant with the cavity field, the strong non-Markovian dynamics in the strong coupling can significantly enhance the work power so that the hybrid system becomes possible as a quantum heat machine.

From the above discussion, we find that thermodynamics quantities, especially the work power and the heat currents, are so sensitive with the non-Markovian dynamics. In the last, we shall look at the strong coupling that the cavity frequency is resonant with the main frequency of the spin ensemble, i.e., $\omega_c = \omega_s$. The driving field is also set to be resonant with the cavity, namely, $\omega_s = \omega_c = \omega_d$. This is indeed the conditions taken in the experiments [51,52]. In this situation, frequency shift is zero (no frequency renormalization) even through it is the strong coupling. In Fig. 9, we show again the same quantities as those in Fig. 8 but for the triple resonances. With the same driving field as given in Fig. 9(a), the internal energy given in Fig. 9(d) reproduces precisely the cavity field intensity measured in experiment [see Fig. 2(b) of Ref. [51]]. Furthermore, as one can see from Figs. 9(c), 9(e), and 9(f), the renormalized driving field, the work power, and the heat current oscillate with spiky positive and negative values. This directly shows how the energy and information (heat) flowing forth and back very rapidly between the cavity and the spin ensemble, as the strongest non-Markovian memory dynamics. Also comparing the results of Figs. 9(e) and 9(f) with those in Figs. 2(c) and 2(d), it shows that the driving field maintains

the work power and heat current do not decay, as one expects for a heat machine.

On the other hand, the above results also show how the strongest non-Markovian dynamics suppress the decoherence of the cavity field, as observed in experiment with such an experiment setup in the strong coupling [51]. It is the heat and work oscillating for long-time forth and back rapidly between the cavity and spin ensemble that leads to the suppression of the decoherence in the strong coupling. Also, the larger magnitudes of the work power and heat current in the resonance indicate the high-energy conversion in this strong-coupling hybrid system, which may serve as a better heat machine. We will leave this problem for further investigation.

IV. CONCLUSIONS

We apply the renormalization theory of quantum thermodynamics we developed recently to investigate transient quantum work power and quantum heat current for a strong-coupling system under external driving. The quantum work arises from the energy renormalization and the renormalized driving field. The heat current is induced by the dissipation and fluctuation dynamics between the system and environment. Without the driving, the work power is contributed only by the energy renormalization of the system but eventually approaches to zero. On the other hand, the driving-induced work power is strongly influenced by the non-Markovian dynamics and makes the system as a non-Markovian heat machine. Furthermore, the heat current consists of the dissipation and the fluctuation heat currents, contributed from dissipation and fluctuations dynamics, respectively. Consequently, the investigation of nonequilibrium energy conversion of heat and work and heat engines should not simply be limited to the problem of how to include the system-environment coupling energy into the system Hamiltonian. It must also take into account the dissipation and fluctuation dynamics induced from the system-environment coupling. With the system Hamiltonian renormalization incorporating the dissipation and fluctuation dynamics together, the energy conversion of heat and work in quantum heat engine can be fundamentally addressed

We study further the transient quantum heat and work in the strong-coupling hybrid system under driving, which consists of a superconducting microwave cavity coupled with a spin ensemble of NV centers in diamond. With the controllability of this hybrid system, one can experimentally tune the coupling strength and the cavity frequency to examine the transient energy conversion. We find that the strong coupling between the cavity and the spin ensemble induces the strong non-Markovian memory effects on the renormalized driving field and the corresponding work power and heat current through the dissipation and fluctuation dynamics of the system. We also find that the energy renormalization in this particular system is negligible. On the other hand, the renormalized driving field is very sensitive when it is resonant with the cavity and the spin ensemble. The driving-induced work power and the heat current are thus enhanced significantly by the non-Markovian dynamics in the resonance conditions. This may provide a new avenue in studying the non-Markovian transient quantum heat and work through quantum engineering for strong-coupling quantum thermodynamics.

[1] C. Jarzynski, equalities and inequalities: Irreversibility and the second law of thermodynamics at the nanoscale, Annu. Rev. Condens. Matter Phys. **2**, 329 (2011).

[2] R. Kosloff, Quantum thermodynamics: A dynamical viewpoint, Entropy **15**, 2100 (2013).

[3] H. N. Xiong, P. Y. Lo, W. M. Zhang, D. H. Feng, and F. Nori, Non-markovian complexity in the quantum-to-classical transition, Sci. Rep. **5**, 13353 (2015).

[4] R. Nandkishore and D. A. Huse, Many-body localization and thermalization in quantum statistical mechanics, Annu. Rev. Condens. Matter Phys. **6**, 15 (2015).

[5] S. Vinjanampathy and J. Anders, Quantum thermodynamics, Contemp. Phys. **57**, 545 (2016).

[6] F. Binder, L. A. Correa, C. Gogolin, J. Anders, and G. Adesso, *Thermodynamics in the Quantum Regime* (Springer, Cham, Switzerland, 2018).

[7] S. Deffner and S. Campbell, *Quantum Thermodynamics: An Introduction to the Thermodynamics of Quantum Information* (Morgan & Claypool, San Rafael, CA, 2019).

[8] P. Talkner and P. Hänggi, Colloquium: Statistical mechanics and thermodynamics at strong coupling: Quantum and classical, Rev. Mod. Phys. **92**, 041002 (2020).

[9] F. L. Xiong and W. M. Zhang, Exact dynamics and thermalization of open quantum systems coupled to reservoirs through particle exchanges, Phys. Rev. A **102**, 022215 (2020).

[10] M. M. Ali, W. M. Huang, and W. M. Zhang, Quantum thermodynamics of single particle systems, Sci. Rep. **10**, 13500 (2020).

[11] G. T. Landi and M. Paternostro, Irreversible entropy production: From classical to quantum, Rev. Mod. Phys. **93**, 035008 (2021).

[12] W. M. Huang and W. M. Zhang, Nonperturbative renormalization of quantum thermodynamics from weak to strong couplings, Phys. Rev. Research **4**, 023141 (2022).

[13] G. Haack and F. Giazotto, Efficient and tunable Aharonov-Bohm quantum heat engine, Phys. Rev. B **100**, 235442 (2019).

[14] M. O. Scully, K. R. Chapin, K. E. Dorfman, M. B. Kim, and A. Svidzinsky, Quantum heat engine power can be increased by noise-induced coherence, Proc. Natl. Acad. Sci. USA **108**, 15097 (2011).

[15] R. Uzdin, A. Levy, and R. Kosloff, Equivalence of Quantum Heat Machines, and Quantum-Thermodynamic Signatures, Phys. Rev. X **5**, 031044 (2015).

[16] J. Roßnagel, O. Abah, F. Schmidt-Kaler, K. Singer, and E. Lutz, Nanoscale Heat Engine Beyond the Carnot Limit, Phys. Rev. Lett. **112**, 030602 (2014).

[17] C. Bergenfeldt, P. Samuelsson, B. Sothmann, C. Flindt, and M. Büttiker, Hybrid Microwave-Cavity Heat Engine, Phys. Rev. Lett. **112**, 076803 (2014).

[18] K. Zhang, F. Bariani, and P. Meystre, Quantum Optomechanical Heat Engine, Phys. Rev. Lett. **112**, 150602 (2014).

[19] J. Roßnagel, S. T. Dawkins, K. N. Tolazzi, O. Abah, E. Lutz, F. Schmidt-Kaler, and K. Singer, A single-atom heat engine, Science **352**, 325 (2016).

[20] G. S. Engel, T. R. Calhoun, E. L. Read, T.-K. Ahn, T. Mančal, Y.-C. Cheng, R. E. Blankenship, and G. R. Fleming, Evidence for wavelike energy transfer through quantum coherence in photosynthetic systems, Nature (London) **446**, 782 (2007).

[21] G. D. Scholes, Coherence in photosynthesis, Nat. Phys. **7**, 448 (2011).

[22] C. Creatore, M. A. Parker, S. Emmott, and A. W. Chin, Efficient Biologically Inspired Photocell Enhanced by Delocalized Quantum States, Phys. Rev. Lett. **111**, 253601 (2013).

[23] K. E. Dorfmana, D. V. Voroninea, S. Mukamelc, and M. O. Scully, Photosynthetic reaction center as a quantum heat engine, Proc. Natl. Acad. Sci. USA **110**, 2746 (2013).

[24] H.-G. Duan, V. I. Prokhorenko, R. J. Cogdell, K. Ashraf, A. L. Stevens, M. Thorwart, and R. J. Dwayne Miller, Nature does not rely on long-lived electronic quantum coherence for photosynthetic energy transfer, Proc. Natl. Acad. Sci. USA **114**, 8493 (2017).

[25] E. Zerah Harush and Y. Dubi, Do photosynthetic complexes use quantum coherence to increase their efficiency? Probably not, Sci. Adv. **7**, eabc4631 (2021).

[26] P. Hänggi, G.-L. Ingold and P. Talkner, Finite quantum dissipation: the challenge of obtaining specific heat, New J. Phys. **10**, 115008 (2008).

[27] G.-L. Ingold, P. Hänggi, and P. Talkner, Specific heat anomalies of open quantum systems, Phys. Rev. E **79**, 061105 (2009).

[28] R. Alicki, The quantum open system as a model of the heat engine, J. Phys. A: Math. Gen. **12**, L103 (1979).

[29] M. Esposito, K. Lindenberg, and C. Van den Broeck, Entropy production as correlation between system and reservoir, New J. Phys. **12**, 013013 (2010).

[30] M. Esposito, M. A. Ochoa, and M. Galperin, Nature of heat in strongly coupled open quantum systems, Phys. Rev. B **92**, 235440 (2015).

[31] U. Seifert, First and Second Law of Thermodynamics at Strong Coupling, Phys. Rev. Lett. **116**, 020601 (2016).

[32] M. Perarnau-Llobet, H. Wilming, A. Riera, R. Gallego, and J. Eisert, Strong Coupling Corrections in Quantum Thermodynamics, Phys. Rev. Lett. **120**, 120602 (2018).

[33] J.-T. Hsiang and B.-L. Hu, Quantum thermodynamics at strong coupling: Operator thermodynamic functions and relations, Entropy **20**, 423 (2018).

[34] M. Campisi, P. Talkner, and P. Hänggi, Fluctuation Theorem for Arbitrary Open Quantum Systems, Phys. Rev. Lett. **102**, 210401 (2009).

[35] L. Nicolin and D. Segal, Quantum fluctuation theorem for heat exchange in the strong coupling regime, Phys. Rev. B **84**, 161414(R) (2011).

[36] A. Dhar, K. Saito, and P. Hänggi, Nonequilibrium density-matrix description of steady-state quantum transport, Phys. Rev. E **85**, 011126 (2012).

[37] C. L. Latune, Steady state in strong system-bath coupling regime: Reaction coordinate versus perturbative expansion, Phys. Rev. E **105**, 024126 (2022)

[38] F. Ivander, N. Anto-Sztrikacs, and D. Segal, Strong system-bath coupling effects in quantum absorption refrigerators, Phys. Rev. E **105**, 034112 (2022).

[39] A. Trushechkin, Quantum master equations and steady states for the ultrastrong-coupling limit and the strong-decoherence limit, arXiv:2109.01888.

[40] P. Gaspard, Scattering approach to the thermodynamics of quantum transport, New J. Phys. **17**, 045001 (2015).

[41] G. E. Topp, T. Brandes and G. Schaller, Steady-state thermodynamics of non-interacting transport beyond weak coupling, Europhys. Lett. **110**, 67003 (2015).

[42] D. Newman, F. Mintert, and A. Nazir, Quantum limit to nonequilibrium heat-engine performance imposed by strong system-reservoir coupling, Phys. Rev. E **101**, 052129 (2020).

[43] Y. Tanimura, Numerically "exact" approach to open quantum dynamics: The hierarchical equations of motion (HEOM), J. Chem. Phys. **153**, 020901 (2020).

[44] M. W. Y. Tu and W. M. Zhang, Non-Markovian decoherence theory for a double-dot charge qubit, Phys. Rev. B **78**, 235311 (2008).

[45] J. Jin, M. W. Y. Tu, W. M. Zhang, and Y. J. Yan, Non-equilibrium quantum theory for nanodevices based on the Feynman-Vernon influence functional, New. J. Phys. **12**, 083013 (2010).

[46] C. U. Lei and W. M. Zhang, A quantum photonic dissipative transport theory, Ann. Phys. **327**, 1408 (2012).

[47] P. Y. Yang and W. M. Zhang, Master equation approach to transient quantum transport in nanostructures, Front. Phys. **12**, 127204 (2017).

[48] H. L. Lai, P. Y. Yang, Y. W. Huang and W. M. Zhang, Exact master equation and non-Markovian decoherence dynamics of Majorana zero modes under gate-induced charge fluctuations, Phys. Rev. B **97**, 054508 (2018).

[49] Y. W. Huang, P. Y. Yang, and W. M. Zhang, Quantum theory of dissipative topological systems, Phys. Rev. B **102**, 165116 (2020).

[50] W. M. Zhang, D. H. Feng, and R. Gilmore, Coherent States: Theory and some applications, Rev. Mod. Phys. **62**, 867 (1990).

[51] S. Putz, D. O. Krimer, R. Amsüss, A. Valookaran, T. Nöbauer, J. Schmiedmayer, S. Rotter, and J. Maje, Protecting a spin ensemble against decoherence in the strong-coupling regime of cavity QED, Nat. Phys. **10**, 720 (2014).

[52] S. Putz, A. Angerer, D. O. Krimer, R. Glattauer, W. J. Munro, S. Rotter, J. Schmiedmayer, and J. Majer, Spectral hole burning and its application in microwave photonics, Nat. Photonics **11**, 36 (2017).

[53] D. O. Krimer, S. Putz, J. Majer, and S. Rotter, Non-Markovian dynamics of a single-mode cavity strongly coupled to an inhomogeneously broadened spin ensemble, Phys. Rev. A **90**, 043852 (2014).

[54] K. T. Chiang and W. M. Zhang, Non-Markovian decoherence dynamics of strong-coupling hybrid quantum systems: A master equation approach, Phys. Rev. A **103**, 013714 (2021).

[55] C.-F. Li, G.-C. Guo, and J. Piilo, Non-Markovian quantum dynamics: What is it good for?, Europhys. Lett. **128**, 30001 (2019).

[56] H.-P. Breuer, Foundations and measures of quantum on-Markovianity, J. Phys. B: At., Mol. Opt. Phys. **45**, 154001 (2012).

[57] A. J. Leggett, S. Chakravarty, A. T. Dorsey, M. P. A. Fisher, A. Garg, and W. Zwerger, Dynamics of the dissipative two-state system, Rev. Mod. Phys. **59**, 1 (1987).

[58] W. M. Zhang, P. Y. Lo, H. N. Xiong, M. W. Y. Tu, and F. Nori, General non-markovian dynamics of open quantum systems, Phys. Rev. Lett. **109**, 170402 (2012).

[59] W. M. Zhang, Exact master equation and general non-Markovian dynamics in open quantum systems, Eur. Phys. J.: Spec. Top. **227**, 1849 (2019).

[60] M. Tavis and F. W. Cummings, Exact solution for an N-molecule-radiation-field Hamiltonian, Phys. Rev. **170**, 379 (1968).

[61] H. Primakoff and T. Holstein, Many-body interactions in atomic and nuclear systems, Phys. Rev. **55**, 1218 (1939).

[62] M. M. Ali, P. Y. Lo, M. W. Y. Tu, and W. M. Zhang, Non-Markovianity measure using two-time correlation functions, Phys. Rev. A **92**, 062306 (2015).

[63] L. P. Kadanoff and G. Baym, *Quantum Statistical Mechanics* (Benjamin, New York, 1962).

[64] L. V. Keldysh, Diagram technique for nonequilibrium processes, Zh. Eksp. Teor. Fiz. **47**, 1515 (1964) [Sov. Phys.–JETP **20**, 1018 (1965)].

[65] K. C. Chou, Z.-B. Su, B.-L. Hao, and L. Yu, Equilibrium and nonequilibrium formalisms made unified, Phys. Rep. **118**, 1 (1985).

[66] G. D. Mahan, *Many-Particle Physics* (Plenum, New York, 1990).

[67] M. E. Peskin and D. V. Schroeder, *An Introduction to Quantum Field Theory* (Addison Wesley, New York, 1995).

[68] M. H. Wu, C. U. Lei, W. M. Zhang, and H. N. Xiong, Non-Markovian dynamics of a microcavity coupled to a waveguide in photonic crystals, Opt. Express **18**, 18407 (2010).